

Hybrid simulations of lateral diffusion in fluctuating membranes

Ellen Reister-Gottfried,* Stefan M. Leitenberger, and Udo Seifert
II. Institut für Theoretische Physik, Universität Stuttgart, 70550 Stuttgart, Germany
(Dated: September 28, 2018)

In this paper we introduce a novel method to simulate lateral diffusion of inclusions in a fluctuating membrane. The regarded systems are governed by two dynamic processes: the height fluctuations of the membrane and the diffusion of the inclusion along the membrane. While membrane fluctuations can be expressed in terms of a dynamic equation which follows from the Helfrich Hamiltonian, the dynamics of the diffusing particle is described by a Langevin or Smoluchowski equation. In the latter equations, the curvature of the surface needs to be accounted for, which makes particle diffusion a function of membrane fluctuations. In our scheme these coupled dynamic equations, the membrane equation and the Langevin equation for the particle, are numerically integrated to simulate diffusion in a membrane. The simulations are used to study the ratio of the diffusion coefficient projected on a flat plane and the intramembrane diffusion coefficient for the case of free diffusion. We compare our results with recent analytical results that employ a preaveraging approximation and analyze the validity of this approximation. A detailed simulation study of the relevant correlation functions reveals a surprisingly large range where the approximation is applicable.

PACS numbers: 87.15.Vv, 87.16.Dg, 87.16.Ac, 05.40.-a

I. INTRODUCTION

During the last decade it has become apparent that lateral diffusion of various components of the cell along the membrane is crucial for several cellular processes, like exo- and endocytosis, cell signaling, or cell movement. To study all these different aspects of lateral diffusion in more detail a whole variety of experimental methods has been developed, including fluorescence recovery after photobleaching (FRAP) [1, 2], single particle tracking (SPT) [3], fluorescence correlation spectroscopy (FCS) [4], or pulsed field gradient nuclear magnetic resonance (pfg-NMR) [5]. While the accuracy of measured diffusion coefficients achieved with these experimental methods can be very high [6], the interpretation of the results is often very difficult. It is, therefore, likely that theoretical calculations and simulations in particular will play a key role in developing a better understanding of diffusive processes in biological membranes.

In order to correctly interpret experimental results it is necessary to analyze what information of the system in which diffusion takes place is documented but also what is neglected or insufficiently regarded during the measurement. Lateral diffusion of proteins in a membrane must not be viewed as diffusion on a flat surface: due to the flexibility of biological membranes lateral diffusion always takes place on curved surfaces, whereby the shape of this surface may also be time dependent. This is an important aspect that needs to be taken into account in the experimental data analysis. However, this turns out to be rather difficult, because not always information on the membrane shape can be acquired. So far several theoretical studies of free diffusion on temporally fixed curved surfaces have been undertaken. One of the first studies of this kind was performed by Aizenbud and Gershon [7] who numerically solved the Smoluchowski equation of free diffu-

sion on a periodic surface. In later studies that include both sophisticated numerical and analytical calculations diffusion on more complicated surfaces is regarded [8, 9, 10, 11, 12]. Recently Schwartz et al. [13] and Sbalzarini et al. [14] simulated free diffusion on surfaces reconstructed from experimental image data. In the latter work, that analyses diffusion in the endoplasmic reticulum (ER), experimental FRAP curves are compared with simulation results. Good agreement is found, however, the authors point out that the evaluation of the FRAP curves assuming the membrane to be flat leads to diffusion coefficients that differ by a factor of about two from the actual intramembrane diffusion coefficient. Furthermore, the experimentally determined diffusion coefficient appears anisotropic while real diffusion along the ER is purely isotropic.

These studies clearly show that the curvature of membranes may not be neglected during the evaluation of experimental data. But even if the shape of the membrane within the measurement volume appears flat on average, the actual shape fluctuates due to thermal activation. These membrane fluctuations have been thoroughly studied. While the fluctuation spectrum of a free and almost flat membrane is easily calculated [15, 16], the influence of various geometric confinements of the membrane have also been regarded. These include the attachment of the membrane to a reference plane via a regular mesh of harmonic springs [17, 18, 19] which resembles a model for the attachment of the cell membrane to the cytoskeleton, a membrane that is close to a flat non-impenetrable surface [20], or the inclusion of active proteins in the membrane, that exert an out-of-plane force on the membrane [21]. Lin and Brown introduced a very powerful method to simulate membrane fluctuations [17, 18, 22], the Fourier space Brownian dynamics algorithm, that allows to add a whole variety of external influences on the membrane. Part of the simulation algorithm introduced in this paper is closely related to this method.

Returning to the movement of proteins along the membrane, it is obvious that membrane fluctuations will influence the measured value of diffusion coefficients. This was first

*Electronic address: reister@theo2.physik.uni-stuttgart.de

pointed out by Gustafsson and Halle [23, 24]. But, although their work is almost ten years old, experimentally diffusion coefficients are still determined by use of the projected flat path particles perform instead of the real path along the membrane. Only recently the quantitative influence of neglecting thermal membrane fluctuations on the measured diffusion coefficients has been estimated both by us and Gov [25, 26]. However, these calculations make use of a preaveraging approximation, that a priori implies that the time it takes a diffusing particle on average to diffuse the length ξ , should be much smaller than the correlation time of a membrane fluctuation mode with wave number $2\pi/\xi$. In this paper we introduce a new algorithm that does not depend on this kind of approximation, because the diffusive motion of a protein along a fluctuating membrane is simulated explicitly. Clearly, the system dynamics is described by two coupled processes: the fluctuations of the membrane and the diffusion of the particle. The simulation of membrane fluctuations is effectively regarded by numerically integrating the equation of motion for a membrane given in the Monge gauge, discretely in time. At each discrete timestep we also update the position of the diffusing particle. To this end the discrete version of the Langevin equation valid for the particle movement is used. Special care needs to be taken regarding this Langevin equation because the movement of the particle depends on the actual shape of the membrane.

As a first test we analyze the height-height correlation function of membrane fluctuations, and compare the simulation results with the analytical result. As mentioned above we have previously calculated the ratio of the measured, or projected, and the intramembrane diffusion coefficient as a function of membrane parameters within a preaveraging approximation.

Using our simulation scheme that does not rely on this kind of approximation we determine the same ratio of diffusion coefficients by analyzing the mean square displacement of diffusing particles. We compare the simulation results with the analytical results and finally discuss the applicability of the preaveraging approximation for situations when diffusive timescales are comparable or smaller than typical membrane time scales by analyzing relevant correlation functions.

The paper is organized as follows: While we introduce the dynamics of membranes in the next section, we explain diffusion on a curved surface in sec. III. Generally diffusion can either be expressed by a Fokker-Planck equation that gives the dynamics of the probability of finding a particle at a certain time and position, or a Langevin equation that corresponds to the equation of motion of the particle position. In secs. III A and III B the Smoluchowski equation, a particular form of the Fokker-Planck equation, and the Langevin equation for diffusion on a curved surface expressed in the Monge gauge are described, respectively. Since simulation results are compared with previous calculations we briefly explain these in sec. IV. After establishing the theoretical foundations necessary for this study we describe our simulation scheme in sec. V with which the results in sec. VI are achieved. In the result section we first analyze pure membrane fluctuations and then determine the ratio of projected and intramembrane diffusion as a function of the membrane parameters bending rigidity

and effective surface and as a function of the intramembrane diffusion coefficient. After the comparison of simulation results with analytical calculations we estimate the limits of the preaveraging approximation in sec. VI C. The paper finishes with some conclusions and an outlook for future work.

II. DYNAMICAL MEMBRANE FLUCTUATIONS

The shape of a membrane without spontaneous curvature, i.e., a membrane that is on average flat and without overhangs, is conveniently described in the Monge gauge. Hereby a position \mathbf{r}^* of the membrane is given by $\mathbf{r}^* \equiv (x, y, h(x, y))$. In the following the vector $\mathbf{r} \equiv (x, y)$ denotes the projected position in the (x, y) -plane. The height function $h(\mathbf{r})$ is the distance between the membrane and the flat (x, y) -plane. The energy of a membrane with bending rigidity κ and effective surface tension σ is given by

$$\mathcal{H}[h(\mathbf{r})] = \int_A d^2\mathbf{r} \left\{ \frac{\kappa}{2} (\nabla^2 h(\mathbf{r}))^2 + \frac{\sigma}{2} (\nabla h(\mathbf{r}))^2 \right\} + \mathcal{H}_1[h(\mathbf{r}), \mathbf{R}] \quad (1)$$

in the Monge gauge [16, 27, 28, 29]. The projected area of the membrane is given by A . A possible energy contribution $\mathcal{H}_1[h(\mathbf{r}), \mathbf{R}]$ is caused by the inserted protein at position $\mathbf{R} \equiv (X, Y)$ and may also depend on the membrane shape. In the following we assume that the system's energy does not depend on the position of the particle and will therefore drop this additional energy term. The dynamics of the membrane is given by the equation of motion for the height function $h(\mathbf{r})$. Because $h(\mathbf{r})$ is not a conserved order parameter the following dynamics applies [16, 17, 22]:

$$\begin{aligned} \frac{\partial h(\mathbf{r}, t)}{\partial t} &= - \int_A d^2\mathbf{r}' \left\{ \Lambda(\mathbf{r} - \mathbf{r}') \frac{\delta \mathcal{H}[h(\mathbf{r}', t)]}{\delta h(\mathbf{r}', t)} \right\} + \xi(\mathbf{r}, t) \\ &= \int_A d^2\mathbf{r}' \left\{ \Lambda(\mathbf{r} - \mathbf{r}') [\kappa \nabla^4 h(\mathbf{r}', t) - \sigma \nabla^2 h(\mathbf{r}', t)] \right\} + \xi(\mathbf{r}, t), \end{aligned} \quad (2)$$

where $\Lambda(\mathbf{r} - \mathbf{r}')$ is an Onsager coefficient and $\xi(\mathbf{r}, t)$ is a fluctuating force that obeys the fluctuation-dissipation theorem:

$$\langle \xi(\mathbf{r}, t) \rangle = 0 \quad (3)$$

$$\langle \xi(\mathbf{r}, t) \xi(\mathbf{r}', t') \rangle = 2k_B T A \Lambda(\mathbf{r} - \mathbf{r}') \delta(t - t'). \quad (4)$$

Applying the following Fourier transform

$$h(\mathbf{k}, t) = \int_A d^2\mathbf{r} h(\mathbf{r}, t) e^{-i\mathbf{k}\cdot\mathbf{r}} \quad (5)$$

$$h(\mathbf{r}, t) = \frac{1}{A} \sum_{\mathbf{k}} h(\mathbf{k}, t) e^{i\mathbf{k}\cdot\mathbf{r}}, \quad (6)$$

the equation of motion for the membrane becomes:

$$\frac{\partial h(\mathbf{k}, t)}{\partial t} = -\Lambda(\mathbf{k}) [\kappa k^4 + \sigma k^2] h(\mathbf{k}, t) + \xi(\mathbf{k}, t), \quad (7)$$

with

$$\begin{aligned} \langle \xi(\mathbf{k}, t) \rangle &= 0 \\ \langle \xi(\mathbf{k}, t) \xi(\mathbf{k}', t') \rangle &= 2k_B T A \Lambda(\mathbf{k}) \delta_{\mathbf{k}, -\mathbf{k}'} \delta(t - t'). \end{aligned} \quad (8)$$

Both the height function $h(\mathbf{r}, t)$ and the random force $\xi(\mathbf{r}, t)$ are real quantities. Therefore the relation $h^*(\mathbf{k}, t) = h(-\mathbf{k}, t)$ applies (for ξ respectively); the asterisk resembles the complex conjugate.

The Onsager coefficient for an almost planar membrane can be derived from the Oseen tensor and takes the following form in Fourier space [15, 16, 30]:

$$\Lambda(\mathbf{k}) = \frac{1}{4\eta k}, \quad (10)$$

with viscosity η of the fluid surrounding the membrane.

Due to the linearity of eq. (7) the height-height correlation function $\langle h(\mathbf{k}, t) h(\mathbf{k}', t') \rangle$, that describes the shape fluctuations of a membrane is easily calculated [16]

$$\begin{aligned} \langle h(\mathbf{k}, t) h(\mathbf{k}', t') \rangle &= \\ \exp \left[-\frac{\kappa k^3 + \sigma k}{4\eta} |t - t'| \right] &\frac{k_B T A}{\kappa k^4 + \sigma k^2} \delta_{\mathbf{k}, -\mathbf{k}'}. \end{aligned} \quad (11)$$

III. DIFFUSION ON CURVED SURFACES

When describing the dynamics of a particle free to diffuse laterally along the membrane one has to bear in mind that the membrane is not flat but curved. The dynamics of the particle is adequately expressed either by a Smoluchowski equation that describes the time evolution of the probability of finding the particle at a certain position, or by a Langevin equation that represents the equation of motion of the particle position. In the following two sections both dynamic equations appropriate for a protein diffusing freely on a curved membrane the shape of which is given in the Monge gauge, will be introduced.

A. Smoluchowski equation

In Cartesian coordinates the Smoluchowski equation for a particle diffusing freely and isotropically on a flat (x, y) -plane is given by

$$\frac{\partial P'(x, y, t)}{\partial t} = D \Delta P'(x, y, t), \quad (12)$$

with the diffusion coefficient D and the probability $P'(x, y, t) dx dy$ of finding the particle in the area element $dx dy$ at position (x, y) . The probability is normalized such that $\int_A dx dy P'(x, y, t) = 1$ applies. On a curved surface the Laplace operator Δ needs to be replaced by the Laplace-Beltrami operator, which is a function of the metric of the surface g and the inverse metric tensor g^{ij} [7, 31]. The resulting Smoluchowski equation takes the form

$$\frac{\partial P(x, y, t)}{\partial t} = D \sum_{i,j} \frac{1}{\sqrt{g}} \partial_i \sqrt{g} g^{ij} \partial_j P(x, y, t). \quad (13)$$

The summations are to be taken over x and y . In the Monge gauge the metric of the surface is given by

$$g \equiv 1 + h_x^2 + h_y^2, \quad (14)$$

with $h_x \equiv \partial_x h(x, y)$, for other subscripts accordingly, and the inverse metric tensor by

$$g^{ij} \equiv \frac{1}{g} \begin{pmatrix} 1 + h_y^2 & -h_x h_y \\ -h_x h_y & 1 + h_x^2 \end{pmatrix}. \quad (15)$$

The probability $\mathcal{P}(x, y, t)$ in eq. (13) is normalized such that $\int_A dx dy \sqrt{g} \mathcal{P}(x, y, t) = 1$ is valid. Assuming that in experiments typically the path of a particle projected on the flat (x, y) -plane is regarded, it makes more sense to evaluate the probability $P(x, y, t) \equiv \frac{1}{\sqrt{g}} \mathcal{P}(x, y, t)$ for which the normalization $\int_A dx dy P(x, y, t) = 1$ applies. To compare results that neglect the curvature of the membrane with those that take it into account correctly, the differences between $P'(x, y, t)$ and $P(x, y, t)$ need to be analyzed. The Smoluchowski equation for $P(x, y, t)$ is

$$\frac{\partial P(x, y, t)}{\partial t} = D \sum_{i,j} \partial_i \sqrt{g} g^{ij} \partial_j \frac{1}{\sqrt{g}} P(x, y, t). \quad (16)$$

The probability of finding the projected position of a particle within the area element $dx dy$ around position (x, y) is now given by $P(x, y, t) dx dy$.

B. Langevin equation

To simulate the movement of a particle in a membrane it is more convenient to use a Langevin equation which describes diffusion on a curved surface. In general it is possible that several different Langevin equations produce the same dynamics of the probability distribution $P(x, y, t)$. In the following we will develop a realization of a Langevin equations in the Ito calculus that leads to the dynamics of eq. (16). Within the Monge description the Langevin equation we wish to develop is ideally the equation of motion of the projected position \mathbf{R} of the particle. The actual particle position is then given by the vector $(X, Y, h(X, Y, t))$. The general form of the Langevin equation in Cartesian coordinates is [32]

$$\frac{\partial R_i}{\partial t} = D b_i + G_{ij} \Gamma_j, \quad (17)$$

where $D b_i$ is the drift term that resembles an external force acting on the particle, and $G_{ij} \Gamma_j$ is a stochastic force with

$$\langle \Gamma_i(t) \rangle = 0 \quad (18)$$

$$\langle \Gamma_i(t) \Gamma_j(t') \rangle = 2\delta_{ij} \delta(t - t'). \quad (19)$$

For the curved system we will develop Langevin equations that obey the form of eq. (17) but where the information on the shape of the surface is incorporated into the drift term b_i and the strength G_{ij} of the stochastic force.

The most general form of a Fokker-Planck equation in two-dimensional Cartesian space is given by [32]

$$\frac{\partial P(x, y, t)}{\partial t} = \left[-\partial_i D_i^{(1)} + \partial_i \partial_j D_{ij}^{(2)} \right] P(x, y, t), \quad (20)$$

with the drift vector $D_i^{(1)}$ and the diffusive tensor $D_{ij}^{(2)}$. Comparing this equation with eq. (16) we can identify

$$D_i^{(1)} = D \frac{1}{\sqrt{g}} (\partial_j (\sqrt{g} g^{ij})) \quad (21)$$

$$D_{ij}^{(2)} = D g^{ij}. \quad (22)$$

Note that the partial derivative in eq. (21) is not applied to $P(x, y, t)$. If we derive the Langevin equations within the Ito calculus the following relationships between the parameters $D_i^{(1)}$ and $D_{ij}^{(2)}$ of the Fokker-Planck equation (20) and the drift term Db_i and the strength G_{ij} of the stochastic force of eq. (17) need to be fulfilled [31, 32]:

$$G_{ij} = \left(D^{(2)^{1/2}} \right)_{ij} = \left(D^{(2)^{1/2}} \right)_{ji} \quad (23)$$

$$Db_i = D_i^{(1)}. \quad (24)$$

Using these relations and the identifications from eqs. (21) and (22) we arrive at the following Langevin equation

$$\begin{aligned} \frac{\partial X(t)}{\partial t} = & D \frac{1}{g^2} [2h_x^2 h_y h_{xy} - h_x h_{xx} (1 + h_y^2) - h_x h_{yy} (1 + h_x^2)] \\ & + \sqrt{D} \frac{1}{g-1} \left(\frac{h_x^2}{\sqrt{g}} + h_y^2 \right) \Gamma_x \\ & + \sqrt{D} \frac{1}{g-1} h_x h_y \left(\frac{1}{\sqrt{g}} - 1 \right) \Gamma_y, \end{aligned} \quad (25)$$

$$\begin{aligned} \frac{\partial Y(t)}{\partial t} = & D \frac{1}{g^2} [2h_x h_y^2 h_{xy} - h_y h_{xx} (1 + h_y^2) - h_y h_{yy} (1 + h_x^2)] \\ & + \sqrt{D} \frac{1}{g-1} h_x h_y \left(\frac{1}{\sqrt{g}} - 1 \right) \Gamma_x \\ & + \sqrt{D} \frac{1}{g-1} \left(\frac{h_y^2}{\sqrt{g}} + h_x^2 \right) \Gamma_y. \end{aligned} \quad (26)$$

Surprisingly, these equations comprise a drift term that is induced by the curvature of the membrane and does not appear in the Langevin equations for free diffusion on a flat plane.

IV. FREE DIFFUSION WITHIN THE PRAEVERAGING APPROXIMATION

Before we turn to the simulation scheme we will give a short introduction to our previous analytical calculations [25] with which we determine the measured, or projected, diffusion coefficient of a protein diffusing freely in a membrane.

The solution of the Smoluchowski equation (16) that describes the time evolution of the probability distribution of the projected position of the diffusing particle, is non trivial because the prefactors containing the metric and the inverse metric tensor are time dependent. If the time τ_ξ it takes a particle to diffuse the length ξ is much longer than the characteristic time $\tau_{\text{memb}, \xi}$ of membrane fluctuations with wavelength ξ we may apply a preaveraging approximation, i.e., we may replace the time dependent prefactors in eq. (16) that contain partial derivatives of $h(\mathbf{r}, t)$ by their thermal averages. The membrane time scale is given by the correlation time in eq. (11) as $\tau_{\text{memb}, \xi} = \eta \xi^3 / (2\pi^3 \kappa)$, while the diffusive timescale is simply given as $\tau_\xi = \xi^2 / 4D$. Comparing these timescales reveals that as long as lengths with

$$\xi \ll \pi^3 \kappa / (2D\eta) \quad (27)$$

are regarded the preaveraging approximation should be valid.

When we average over the prefactors of eq. (16) we find that most terms vanish and the Smoluchowski equation simplifies considerably. Taking into account only leading order prefactors it reads:

$$\begin{aligned} \frac{\partial P(x, y, t)}{\partial t} = D \left[\left\langle \frac{1 + h_y^2}{g} \right\rangle \frac{\partial^2 P(x, y, t)}{\partial x^2} \right. \\ \left. + \left\langle \frac{1 + h_x^2}{g} \right\rangle \frac{\partial^2 P(x, y, t)}{\partial y^2} \right]. \end{aligned} \quad (28)$$

In an isotropic membrane the two remaining thermal averages are both equal and therefore the Smoluchowski equation takes the form applicable for diffusion on a flat surface, cf. (12), but now with a new diffusion coefficient D_{proj} . The ratio of D_{proj} that would be measured in experiments, and the actual intramembrane coefficient D is given by:

$$\frac{D_{\text{proj}}}{D} = \frac{1}{2} \left(1 + \left\langle \frac{1}{g} \right\rangle \right). \quad (29)$$

By use of the relation $1/g = \int_0^\infty d\alpha \exp[-\alpha g]$ and the Helfrich Hamiltonian (1) this ratio becomes:

$$\begin{aligned} \frac{D_{\text{proj}}}{D} = & \frac{1}{2} + \frac{1}{2} \int_0^\infty d\alpha \exp \left[-\frac{1}{2} \sum_{\substack{k_x, k_y \\ |\mathbf{k}| < q_m}} \ln \left(1 + \frac{2\alpha}{\beta L^2 \kappa k^2 + \sigma} \right) \right]. \end{aligned} \quad (30)$$

A cutoff wavenumber $q_m \sim a$ needs to be introduced that is proportional to the inverse of the microscopic length scale a in the system. As we will see later, in the simulations this microscopic length scale corresponds to the lattice spacing. For a more detailed discussion of the numerical evaluation and the results of this equation we refer the reader to our previous work [25].

Instead of regarding the preaveraging approximation in the Smoluchowski equation it may also be applied in the Langevin equations (25), (26). The averaging process leads to

a vanishing drift term; the calculation of the the mean square displacement and the subsequent derivation of the effective diffusion coefficient leads to $D_{\text{proj}}/D = \langle G_{xx}^2 + G_{yy}^2 \rangle / 2D = (1 + \langle 1/g \rangle) / 2$. This is the same result as eq. (29).

V. SIMULATION SCHEME

The analytical calculations in the last section were performed within a preaveraging approximation. In the present work we do not apply this approximation, but rather simulate the equation of motion for the membrane (2) and the Langevin equations (25) and (26) for the protein movement. The simulation scheme that we will introduce during the next paragraphs resembles the effective evaluation of this coupled set of dynamic equations by means of discrete numerical integration in time.

First let us turn to the numerical evaluation of the time evolution of the membrane shape. If we regard eq. (7) and assume periodic boundary conditions it is obvious that the numerical integration is most effectively implemented in Fourier space because the evolution of the height function modes $h(\mathbf{k}, t)$ takes place independently of each other. If the diffusion of the protein were not taken into account the whole time evolution of the membrane shape could be performed in \mathbf{k} -space. However, the real space representation $h(\mathbf{r}, t)$ becomes necessary to develop the position of the protein. Due to the periodic boundary conditions \mathbf{k} -vectors are of the form $\mathbf{k} = 2\pi(l, m)/L$ with $A = L^2$. Because in real space $h(\mathbf{r}, t)$ is expressed on a quadratic lattice of $N \times N$ lattice sites the restriction $-N/2 < l, m \leq N/2$ applies. The lattice spacing a is given by $a \equiv L/N$.

When numerically implementing eq. (7) one must remember that $h(\mathbf{k}, t)$ may be a complex number with a real part $h_r(\mathbf{k}, t)$ and an imaginary part $h_i(\mathbf{k}, t)$ such that $h(\mathbf{k}, t) = h_r(\mathbf{k}, t) + ih_i(\mathbf{k}, t)$. Both for the real and the imaginary part an equation of motion is necessary. The numerical equations that are used in the simulations to develop the membrane shape during a timestep Δt are of the form

$$\begin{aligned} h_{r/i}(\mathbf{k}, t) &= h_{r/i}(\mathbf{k}, t - \Delta t) \\ &+ \Delta t \frac{1}{4\eta k} [\kappa k^4 + \sigma k^2] h_{r/i}(\mathbf{k}, t - \Delta t) \\ &+ \sqrt{\lambda k_B T A \Delta t / (4\eta k)} r. \end{aligned} \quad (31)$$

The random number r is Gaussian and therefore $\langle r \rangle = 0$ and $\langle r^2 \rangle = 1$ applies. The factor λ in the random term is either 1 or 2 as we will now explain: Due to $h(\mathbf{r}, t)$ and $\xi(\mathbf{r}, t)$ being real quantities not all modes have an imaginary part. In particular modes with wave vectors $\mathbf{k} = 2\pi(l, m)/L$ with $(l, m) = (0, 0), (0, N/2), (N/2, 0), (N/2, N/2)$ are purely real, while all others are complex. In order to fulfill the fluctuation dissipation theorem from eq. (9) the four purely real modes only have an equation of motion for the real part with $\lambda = 2$, while all other independent modes have two equations of motion, one for the real and one for the imaginary part, each with $\lambda = 1$. The real and the imaginary part of $\xi(\mathbf{k}, t)$ are assumed not to be correlated. Note that not all modes are

independent, because $h(\mathbf{r}, t)$ is a real function. Only a set of independent modes is updated via (31), while the dependent modes are set such that $h(\mathbf{k}, t) = h^*(-\mathbf{k}, t)$.

Regarding the random term in eq. (31) it becomes evident that it diverges for $k = 0$ due to the Onsager coefficient $\Lambda(\mathbf{k})$. The mode $h(\mathbf{k} = 0, t)$ is a measure for the distance between the center of mass of the membrane and the flat (x, y) -plane. Therefore, fluctuations of $h(\mathbf{k} = 0, t)$ just describe a movement of the membrane as a whole. Such movement of the center of mass is of no relevance for the membrane and diffusive properties of interest in this work, so we keep $h(\mathbf{k} = 0, t) = 0$ fixed at all times.

So far the simulation scheme is rather similar to the *Fourier space Brownian dynamics* method introduced earlier by Lin and Brown [17, 18, 22]. But in our simulations we additionally take into account the diffusion of a freely diffusing particle along the curved surface given by the membrane shape. After an update in the membrane shape using eqs. (31) we will now update the position of the diffusing particle by using a discrete version of eqs. (25) and (26) [31, 32]:

$$\begin{aligned} X(t + \Delta t) &= X(t) \\ &+ D \frac{1}{g^2} [2h_x^2 h_y h_{xy} - h_x h_{xx} (1 + h_y^2) - h_x h_{yy} (1 + h_x^2)] \Delta t \\ &+ \sqrt{D} \frac{1}{g - 1} \left(\frac{h_x^2}{\sqrt{g}} + h_y^2 \right) \sqrt{2\Delta t} r_x \\ &+ \sqrt{D} \frac{1}{g - 1} h_x h_y \left(\frac{1}{\sqrt{g}} - 1 \right) \sqrt{2\Delta t} r_y. \end{aligned} \quad (32)$$

For $Y(t)$ the corresponding equation is valid. Hereby we use $h_x(\mathbf{R}(t), t)$, for all other partial derivatives of h accordingly, at the position of the particle $\mathbf{R}(t)$ at time t . The random numbers r_x and r_y are again Gaussian with $\langle r_i \rangle = 0$ and $\langle r_i r_j \rangle = \delta_{ij}$. This equation clearly describes an off-lattice movement of the particle. It is also conceivable to simulate the protein movement through a random walk on the lattice used for the membrane. In such a scheme we would check the probability of a particle moving to a neighboring lattice site within a timestep Δt and then decide whether the particle is to hop. In biological systems, however, the time it takes a particle to diffuse the length of a lattice spacing a in the simulation is much larger than the typical timescale of membrane fluctuations with wave length a . This would typically lead to significant changes in the membrane shape before a particle jump is successful. Therefore, the off-lattice version of the particle's random walk is much more favorable, although the partial derivatives of h need to be extrapolated to the position of the particle. This is realized by the following procedure: Multiplying $h(\mathbf{k}, t)$ with the appropriate \mathbf{k} -vectors and subsequently performing the Fourier backtransform, we arrive at the first and second partial derivatives of $h(\mathbf{r}, t)$ with respect to x and y . All discrete Fourier transformations necessary for the simulations are effectively implemented using the FFTW routines [33]. Assume that the protein is to be found somewhere between the four lattice sites $(i, j), (i + 1, j), (i, j + 1)$, and $(i + 1, j + 1)$, with $0 \leq i, j \leq N - 1$. The quantity $A(\mathbf{R})$ to be extrapolated to the particle position is given at the lattice

sites by $A(i, j)$, $A(i + 1, j)$, etc. The distance between the particle and the line connecting (i, j) and $(i, j + 1)$ is to be μa and the distance between particle and the line connecting (i, j) and $(i + 1, j)$ is νa . The linearly extrapolated value of A at the particle position $\mathbf{R} = (a(i + \mu), a(j + \nu))$ is calculated by use of:

$$\begin{aligned} A(\mathbf{R}) = & A(i, j) \\ & - \nu a(A(i, j) - A(i, j + 1)) - \mu a(A(i, j) - A(i + 1, j)) \\ & + \mu \nu a^2(A(i, j) - A(i + 1, j)) \\ & + A(i + 1, j + 1) - A(i, j + 1) \end{aligned} \quad (33)$$

After all the necessary quantities have been determined at position \mathbf{R} the new particle position is calculated with eq. (32). During the timestep of course also the shape of the membrane will change. This is accounted for by employing eq. (31) in the next computational step to get $h(\mathbf{k}, t + \Delta t)$. Then we again update the particle position and so on. Repeating the two step process of membrane shape update and particle movement makes out our simulation scheme.

Instead of simulating the diffusion of one particle in one membrane it possible to insert several particles into the membrane that do not interact with each other. For each particle a separate Langevin equation needs to be evaluated, but only one membrane equation of motion. Since the Fourier transform of the membrane configuration is the most time consuming element of the code, the insertion of more than one particle saves computing time. However, the average distance between the particles should be sufficiently large in order for the particle paths to be independent. Results presented in sections VI B and VI C follow from averaging over 2500 paths in 100 different membranes. In each independent membrane 25 particles, that do not interact with each other, are allowed to diffuse.

All simulation results presented in this paper were performed on a 50×50 lattice. If we assume (arbitrarily) that the lattice spacing a corresponds to 10nm the system size is $L = 0.5\mu\text{m}$. The viscosity η of the water surrounding the membrane is $\eta = 10^{-9}\text{Js/cm}^3$. With the above chosen lattice spacing a and the temperature $T = 300\text{K}$, the viscosity used in the Onsager coefficient of the simulations is $\eta = 2.4 \times 10^{-7}k_B T s/a^3$.

The choice of the appropriate timestep Δt is determined by two timescales, namely the smallest timescale of membrane fluctuations $\tau_{\text{memb},\text{min}}$ and the time $\tau_{\text{diff},a}$ it takes a particle on average to diffuse a lattice spacing a . Only if Δt is significantly smaller than $\tau_{\text{memb},\text{min}}$ then the evolution of the membrane shape will be numerically stable. The membrane timescale is given by $\tau_{\text{memb},\text{min}} = 4\eta/(\kappa k_{\text{max}}^3 + \sigma k_{\text{max}})$, cf. eq. (11). The maximum wave number $k_{\text{max}} = \sqrt{2}\pi/a$ is determined by the minimal microscopic length scale of the system, i.e., in simulations the lattice spacing a . Additionally the average length a particle moves during Δt needs to be much shorter than a , because we regard the membrane shape only right at the beginning of the jump. If the jump is too big, the actual particle path along the membrane is not taken into account with the necessary accuracy. The diffusive timescale is determined by $\tau_{\text{diff},a} = a^2/4D$. To perform the simulations Δt should be considerably smaller than both $\tau_{\text{memb},\text{min}}$

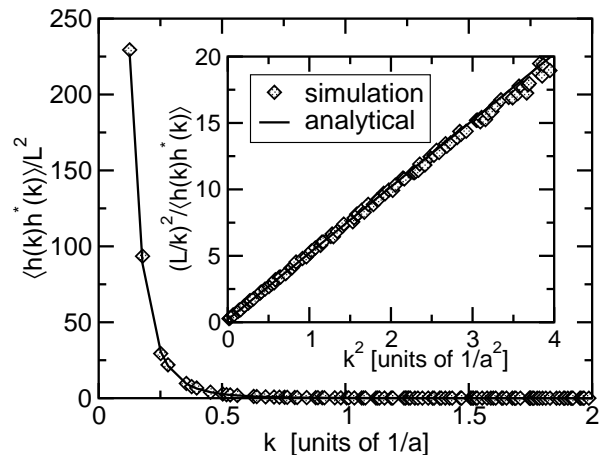


FIG. 1: Height-height correlation function $\langle h(\mathbf{k})h^*(\mathbf{k}) \rangle$ as a function of wave number k (in units of $1/a$). To illustrate the agreement between the analytical and the simulation result for larger k values, we plot $k^2/\langle h(\mathbf{k})h^*(\mathbf{k}) \rangle$ as a function of k^2 in the inset. The simulation results, symbolized by the diamond symbols, were obtained by averaging over 250 independent membrane configurations created during runs with dimensionless physical parameters $\beta\kappa = 5$ and $\beta\sigma L^2 = 500$ on a 50×50 lattice. The numerical timestep was $\Delta t = 1.7 \times 10^{-10}\text{s}$.

and $\tau_{\text{diff},a}$. Timesteps Δt used in the presented simulations range from $5 \times 10^{-10}\text{s}$ to $2 \times 10^{-9}\text{s}$. Typical simulation runs comprise $\sim 2 \times 10^6$ timesteps which took approximately 30-35 minutes on a 64 node Beowulf cluster with Pentium IV, 3.2 GHz processors.

VI. RESULTS

A. Validation of membrane fluctuations

After developing a simulation code it is always necessary to test it by comparing its results with results previously obtained with another method. In this section we will show that the evolution of the membrane shape results in the membrane fluctuations given by eq. (11) that follow analytically for a membrane with the Helfrich energy (1) and the Onsager coefficient of eq. (10).

In fig. 1 we display the equal time correlation function $\langle h_r^2(\mathbf{k}, t) + h_i^2(\mathbf{k}, t) \rangle$ as a function of $k \equiv |\mathbf{k}|$ for $\beta\kappa = 5$ and $\beta\sigma L^2 = 500$. This corresponds to a surface tension on the order of $8 \times 10^{-3}\text{mJ/m}^2$. Typical values for the dimensionless bending rigidity $\beta\kappa$ of lipid bilayer membranes are between 1 and 50.

If we compare the simulation results with the analytical result that is given by the solid line we see a good agreement for small wave numbers. For higher k values it is more convenient to plot $k^2/\langle h_r^2(\mathbf{k}, t) + h_i^2(\mathbf{k}, t) \rangle$ as a function of k^2 , which is done in the inset. The linear behavior expected from the analytical calculations is well reproduced by the simulations.

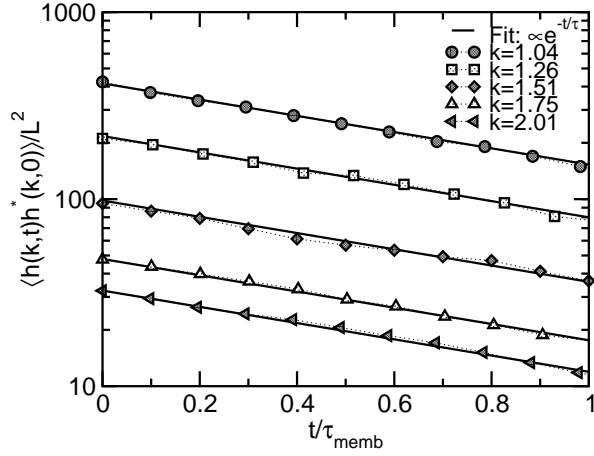


FIG. 2: Time correlation function $\langle h(\mathbf{k}, t)h^*(\mathbf{k}, 0) \rangle$ as a function of the dimensionless time $t/\tau_{\text{memb}}(k)$ for the given values of k . The correlation time $\tau_{\text{memb}}(k) = 4\eta/(\kappa k^3 + \sigma k)$ is given by eq. (11). Symbols are results from the simulations, while straight lines resemble fits $\propto \exp[-t/\tau_{\text{memb}}]$.

In order to test the time correlations of the membrane fluctuations we plot the correlation function $\langle h(\mathbf{k}, t)h^*(\mathbf{k}, 0) \rangle$ as a function of the dimensionless time $t/\tau_{\text{memb}}(k)$ for several randomly chosen wave numbers in fig. 2. The same parameters as in fig. 1 were used. The exponential fits $\propto \exp[-t/\tau_{\text{memb}}]$ to the simulation results reveal a good agreement between the analytical correlation times and the results obtained from our numerical membrane update scheme.

B. Free membrane-bound diffusion

In the previous section we showed that our simulation scheme reproduces membrane fluctuations correctly. In this section we show that it is also capable of adequately describing the diffusion of a protein in the membrane.

To determine the projected diffusion coefficient in the simulations we use the relation $\langle (\mathbf{R}(t) - \mathbf{R}(0))^2 \rangle = 4D_{\text{proj}}t$. The mean square displacement $\langle \Delta \mathbf{R}^2(t) \rangle \equiv \langle (\mathbf{R}(t) - \mathbf{R}(0))^2 \rangle$ as a function of time is determined from the simulations by averaging over a large number of independent particle paths. In fig. 3 we show $\langle \Delta \mathbf{R}^2(t) \rangle / 4D$ as a function of time for the given values of $\beta\kappa$ and $\sigma = 0$. The chosen intramembrane diffusion coefficient is $D = 10^5 a^2/s$; this corresponds to an experimental value of $D = 10^{-7} \text{cm}^2/s$. The results evidently show a linear increase of $\langle \Delta \mathbf{R}^2(t) \rangle$ with time. Furthermore, the comparison of the simulation results with the line that gives the expected mean square displacement if the membrane were flat displays that the projected diffusion coefficient is smaller than the actual intramembrane diffusion coefficient. This is of course expected and also seen in the result of eq. (29), because membrane fluctuations increase the actual path of the protein.

The slope of the linear fit to the simulation results some of which are displayed in fig. 3 corresponds to the ratio D_{proj}/D . In fig. 4 we plot D_{proj}/D resulting from the simulations and

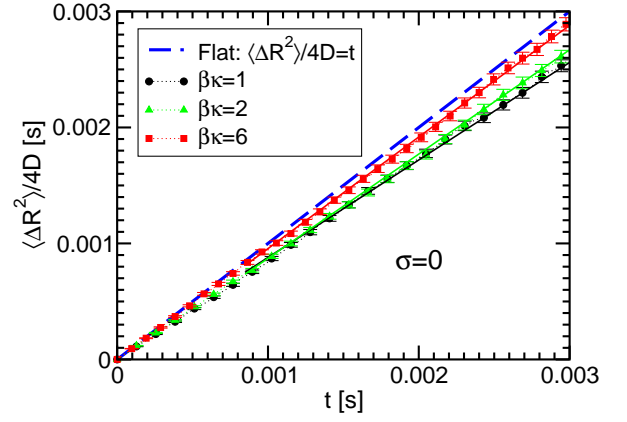


FIG. 3: (Color online) Elucidation how D_{proj} is determined from simulation results (symbols): the averaged mean square displacement $\langle \Delta \mathbf{R}^2(t) \rangle / 4D$ is plotted as a function of time. The error bars correspond to the standard error of averaging. The slopes of linear fits (solid lines) to these results determine the diffusion coefficient. The projected diffusion coefficient on a fluctuating membrane is always smaller than on a flat plane (thick dashed line).

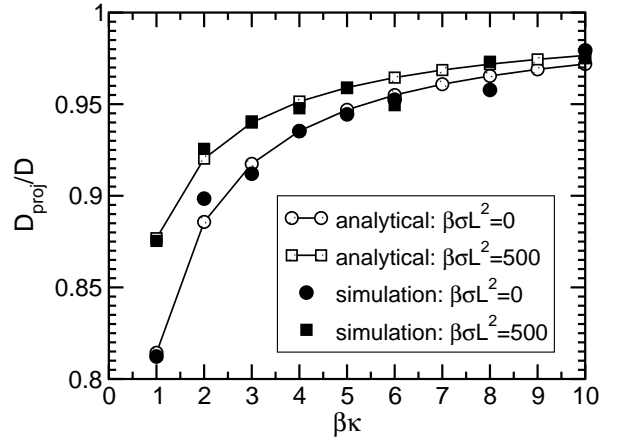


FIG. 4: Comparison of simulation and analytical results for D_{proj}/D as a function of bending rigidity $\beta\kappa$ for the two given effective tensions. Good agreement is observed.

the numerical evaluation of the integral in eq. (30) as a function of bending rigidity $\beta\kappa$ both for vanishing tension and $\beta\sigma L^2 = 500$. Both simulations and preaveraging calculations show that for small bending rigidity and small tension the difference between projected and actual diffusion coefficient becomes more and more pronounced. This result is plausible: decreasing tension σ and bending rigidity κ leads to stronger membrane fluctuations. The difference between actual and projected particle path becomes bigger and therefore the fluctuation effect is enhanced. If the system size is increased, not shown here, this also leads to an increase in fluctuation strength. The comparison of simulation and analytical results displays a very good overall agreement.

Results in fig. 4 were achieved for a single diffusion coef-

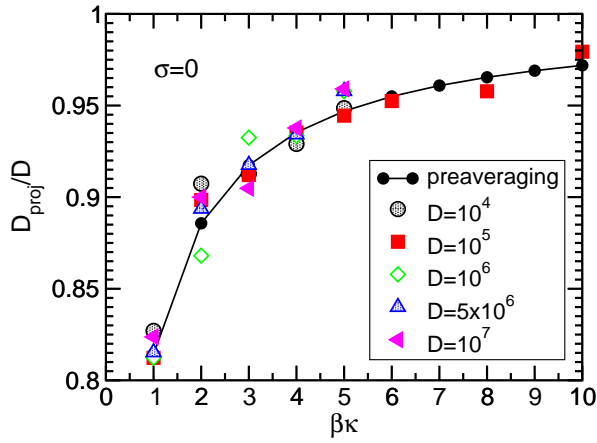


FIG. 5: (Color online) Ratio of the projected to the intramembrane diffusion coefficient D_{proj}/D as a function of $\beta\kappa$ for various diffusion coefficients (given in units of a^2/s) and $\sigma = 0$. Simulation results for all D cannot be distinguished from the preaveraging result.

efficient D . To study the influence of the intramembrane diffusion coefficient we also perform simulations for five different coefficients $D = 10^4, 10^5, 10^6, 5 \times 10^6, 10^7 a^2/s$ and $\sigma = 0$. In fig. 5 we display the ratio D_{proj}/D as a function of $\beta\kappa$ for all used D as derived from the average mean square displacement $\langle \Delta \mathbf{R}^2(t) \rangle$ of the diffusing particles. The results show that D_{proj}/D is seemingly independent of the diffusion coefficient D : for all values of D a good agreement of the simulation results is observed. Comparing the simulation results with the analytical result invoking the preaveraging approximation we also find that the agreement is very good. But this is rather surprising: a priori the preaveraging approximation should only be applicable if the time it takes a particle to diffuse the length ξ is much larger than the correlation time of membrane fluctuations with wavelength ξ . This is expressed in eq. (27) where we have a crossover length scale $\xi_{\text{co}} \equiv \pi^3 \kappa / (2D\eta) \simeq 6 \times 10^7 \beta\kappa / D$. If diffusion on length scales below ξ_{co} is analyzed the preaveraging approximation should lead to good agreement, while one would expect to see a change for larger length scales. For the smallest regarded diffusion coefficients ξ_{co} is on the order of $10^3 a$. With a system length of $L = 50a$ all lengths in the system are below the crossover length scale and therefore the agreement of the simulation results with the preaveraging result, as seen in figs. 4 and 5, is expected. For the largest regarded D the crossover length is on the order of $10a$. Thus there are very many membrane fluctuation modes in the system with wave lengths larger than ξ_{co} . In this case we would have expected the interplay of membrane and diffusive timescales to be observable in the effective diffusion coefficient. However, fig. 5 shows that this is not the case. To understand why the preaveraging approximation leads to good agreement with explicit simulations even for large D , it is necessary to study the correlations of the drift term in the Langevin equations (25) and (26) that is caused by the metric of the system. This is the subject of the following section where we discuss the validity

of the preaveraging approximation.

C. Validity of the preaveraging approximation

The last section had the unexpected outcome that the analytical calculation within the preaveraging approximation describes particle diffusion well even when the diffusion coefficient is so large that one would assume this approximation to break down. In this section we study in more detail the validity of the preaveraging approximation.

To this end it is helpful to regard the Langevin equations (25) and (26) governing particle diffusion. The diffusion coefficient is defined through the mean square displacement of the diffusing particle. Using eq. (17) we can formally write the mean square displacement as

$$\begin{aligned} \langle \Delta \mathbf{R}^2(t) \rangle = & D^2 \int_0^t d\tau \int_0^t d\tau' \left\{ \sum_i \langle b_i(\mathbf{R}(\tau); \tau) b_i(\mathbf{R}(\tau'); \tau') \rangle \right\} \\ & + 2 \sum_i \langle G_{ii}^2 \rangle t. \quad (34) \end{aligned}$$

The last term that is linear in time t coincides with the preaveraging result, because $\langle G_{xx}^2 + G_{yy}^2 \rangle / 2D = (1 + \langle 1/g \rangle) / 2$, see eq. (29). Hence the diffusion coefficient derived through $\langle \Delta \mathbf{R}^2(t) \rangle / 4t$ gets an additional term caused by the correlations of the drift term. If we are interested in the ratio of the projected and the actual diffusion coefficient it may be written as the sum of two terms $D_{\text{proj}}/D = D_{\text{proj,preav}}/D + D_{\text{proj,drift}}/D$, with the additional contribution

$$\begin{aligned} \frac{D_{\text{proj,drift}}}{D} = & \frac{1}{2t} D \int_0^t d\tau \int_0^t d\tau' \{ \langle b_x[h(\mathbf{R}(\tau); \tau)] b_x[h(\mathbf{R}(\tau'); \tau')] \rangle + \\ & \langle b_y[h(\mathbf{R}(\tau); \tau)] b_y[h(\mathbf{R}(\tau'); \tau')] \rangle \}, \quad (35) \end{aligned}$$

with

$$\begin{aligned} b_x[h] \equiv & \frac{1}{g^2} [2h_x^2 h_y h_{xy} - h_x h_{xx} (1+h_y^2) - h_x h_{yy} (1+h_x^2)], \\ b_y[h] \equiv & \frac{1}{g^2} [2h_y^2 h_x h_{xy} - h_y h_{yy} (1+h_x^2) - h_x h_{xx} (1+h_y^2)]. \quad (36) \end{aligned}$$

In order to estimate this contribution we calculate the functions $\langle b_x(\mathbf{R}(\tau); \tau) b_x(\mathbf{R}(\tau + \Delta\tau); \tau + \Delta\tau) \rangle$ and $\langle b_y(\mathbf{R}(\tau); \tau) b_y(\mathbf{R}(\tau + \Delta\tau); \tau + \Delta\tau) \rangle$ from our simulation data for the five previously regarded diffusion coefficients. Note that the correlations do not only depend on the pure time interval $|\tau - \tau'|$ but also on the distance $|\mathbf{R}(\tau) - \mathbf{R}(\tau')|$ the particle travels during this time interval. The correlation functions are displayed in the top and bottom panels of fig. 6 as a function of $\Delta\tau$ for $\beta\kappa = 1$ and $\beta\kappa = 2$. In this whole section we set the effective surface tension $\sigma = 0$. We find that the correlation function is overall smaller

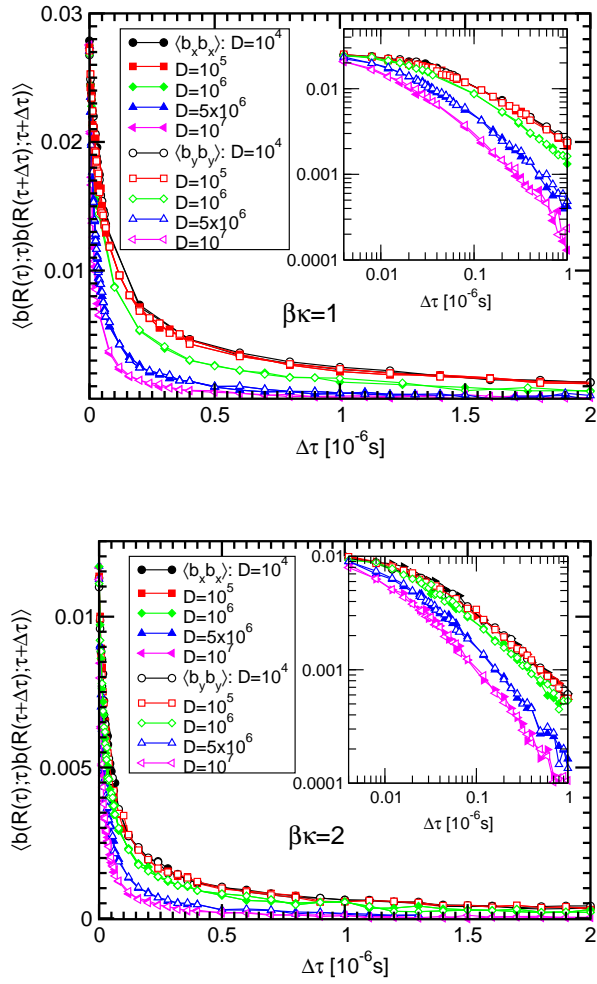


FIG. 6: (Color online) Correlation functions $\langle b_x(\mathbf{R}(\tau); \tau) b_x(\mathbf{R}(\tau + \Delta\tau); \tau + \Delta\tau) \rangle$ (solid symbols) and $\langle b_y(\mathbf{R}(\tau); \tau) b_y(\mathbf{R}(\tau + \Delta\tau); \tau + \Delta\tau) \rangle$ (white symbols) as a function of $\Delta\tau$ for $\beta\kappa = 1$ (top panel) and $\beta\kappa = 2$ (bottom panel). Different symbols apply for different diffusion coefficients (given in units of a^2/s). The insets display the same results as double logarithmic plots.

for larger $\beta\kappa$ as is expected. This means that the larger the bending rigidity κ or the effective tension σ , not shown here, the less important is the contribution caused by the drift term. The expectation for an isotropic system that the correlation functions $\langle b_x(\mathbf{R}(\tau); \tau) b_x(\mathbf{R}(\tau + \Delta\tau); \tau + \Delta\tau) \rangle$ and $\langle b_y(\mathbf{R}(\tau); \tau) b_y(\mathbf{R}(\tau + \Delta\tau); \tau + \Delta\tau) \rangle$ coincide, is also fulfilled. Furthermore, a faster decrease of the correlation function with increasing diffusion coefficient D is observed. The decrease of the correlation function with time $\Delta\tau$ is determined by two processes: the change in membrane shape and the movement of the particle along the membrane. If the particle did not diffuse, i.e., $D = 0$, the displayed correlation functions would still decrease with increasing the time interval due to the evolution of the membrane shape. This contribution to the decrease obviously does not depend on how fast the particle diffuses within the membrane, but only depends on membrane parameters like bending rigidity κ or surface tension σ .

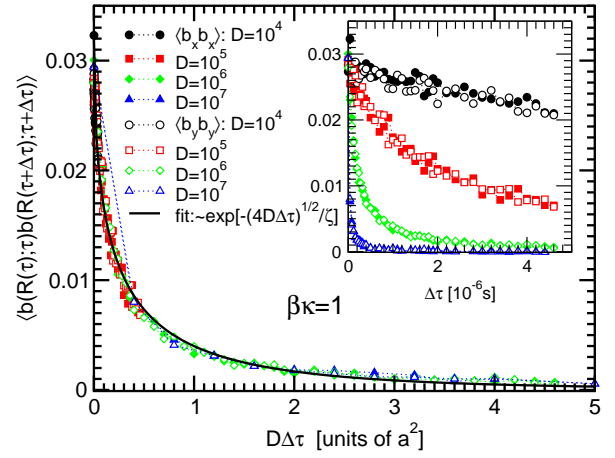


FIG. 7: (Color online) Correlation functions $\langle b_x(\mathbf{R}(\tau); \tau) b_x(\mathbf{R}(\tau + \Delta\tau); \tau + \Delta\tau) \rangle$ (solid symbols) and $\langle b_y(\mathbf{R}(\tau); \tau) b_y(\mathbf{R}(\tau + \Delta\tau); \tau + \Delta\tau) \rangle$ (white symbols) as a function of $D\Delta\tau$ and $\Delta\tau$ (inset) resulting from diffusion on 100 different quenched membranes with 25 particles each for $\beta\kappa = 1$. Different symbols apply for different diffusion coefficients.

In the other extreme when membrane time scales τ_{memb} approach infinity, and the particle diffuses on a fixed membrane shape, the decrease of the correlation function is determined by the distance a particle travels during a fixed time interval. This is shown in fig. 7 for $\beta\kappa = 1$, where we display the correlation functions $\langle b_i(\mathbf{R}(\tau); \tau) b_i(\mathbf{R}(\tau + \Delta\tau); \tau + \Delta\tau) \rangle$ for particles diffusing on different quenched membranes over which we average afterwards. The “quenched” configurations used in the simulations are obtained by evolving the membrane shape for such a long time that thermal equilibrium has been reached. Regarding the correlation functions as a function of time we see that the smaller the diffusion coefficient the slower the decrease of the correlations. Multiplying $\Delta\tau$ with the diffusion coefficient leads to a perfect match of all four lines. This is a clear indication that the correlation function depends only on the average distance $\sqrt{4D\Delta\tau}$ a particle travels during a certain time. The thick solid line is the result of an exponential fit $\propto \exp(-\sqrt{4D\Delta\tau}/\zeta)$; the correlation length for $\beta\kappa = 1$ is given by $\zeta \simeq 1.0a$.

If we return to fig. 6 where both the membrane and the particle are moving, it is now understandable that an increasing diffusion coefficient leads to a faster decrease of the correlation functions. An analytic form for the observed correlation functions could not be found.

In order to estimate the additional contribution to the projected diffusion coefficient the correlation functions need to be integrated according to eq. (34). Regarding the results in fig. 6 it is obvious that the double integration of the correlation functions $\langle b_i(\mathbf{R}(\tau); \tau) b_i(\mathbf{R}(\tau + \Delta\tau); \tau + \Delta\tau) \rangle$ in time will cause a slower increase with time for large D . However, the additional contribution $D_{\text{proj,drift}}/D$ is given by multiplying this integral by D . The additional mean square displacement $\langle \Delta\mathbf{R}_{\text{drift}}^2(t) \rangle / 4D$ resulting from the numerical integration of the results in fig. 6 is displayed in fig. 8 for $\beta\kappa = 1$.

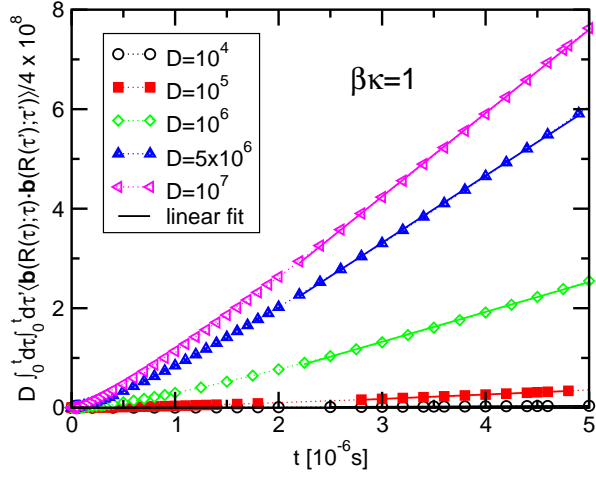


FIG. 8: (Color online) Additional mean square displacement $\langle \Delta \mathbf{R}_{\text{drift}}^2(t) \rangle / 4D$ as a function of time t for $\beta\kappa = 1$ as derived by numerically evaluating the first term of eq. (34).

For all regarded diffusion coefficients we find a linear behavior for large times t . Furthermore, the slope becomes larger for increasing D . In other words the influence of the drift term becomes more pronounced the faster the particle diffuses compared to the fluctuations of the membrane.

In this context it is interesting to check whether the additional contribution is finite for an infinite intramembrane diffusion coefficient. For very large diffusion coefficients the membrane will appear almost stiff for the moving particle. This corresponds to the situation regarded in fig. 7, where we found that the correlation function is well described by an exponential function $\langle b_i(\mathbf{R}(\tau); \tau) b_i(\mathbf{R}(\tau + \Delta\tau); \tau + \Delta\tau) \rangle \simeq \langle b_i^2(\mathbf{R}(\tau); \tau) \rangle \exp[-\sqrt{4D\Delta\tau}/\zeta]$. For this particular function eq. (35) is easily evaluated. In the limit of large times t we find $D_{\text{proj,drift}}/D = \langle b_i^2(\mathbf{R}(\tau); \tau) \rangle \zeta^2 / 2$. Thus $D_{\text{proj,drift}}/D$ is independent of D , and only involves membrane parameters. It therefore remains finite. For $\beta\kappa = 1$ the largest possible increase of D_{proj}/D is approximately $\simeq 0.015$.

The additional terms to the ratio of projected to intramembrane diffusion coefficient $D_{\text{proj,drift}}/D$ resulting from fits to $\langle \Delta \mathbf{R}_{\text{drift}}^2(t) \rangle$, see fig. 8, are displayed in fig. 9. Although an increase in D causes a larger additional term we still see that for the regarded diffusion coefficients that are much larger than those experimentally observed in experiments, the additional term is always more than two orders of magnitudes smaller than $D_{\text{proj,preav}}/D$. For $D = 10^7 \text{a}^2/\text{s}$ the numerically determined value of $D_{\text{proj,drift}}/D$ agrees reasonably well with the previous estimate for infinite D . Surprisingly, for situations when one expects the preaveraging approximation to break down, it still gives reliable results. Even for infinite diffusion coefficients the results for the projected diffusion coefficient calculated within the preaveraging approximation only differ from the actual values by less than two percent for experimentally accessible membranes.

After this discussion we can understand why our simulation runs agree well with the preaveraging result for all D , as

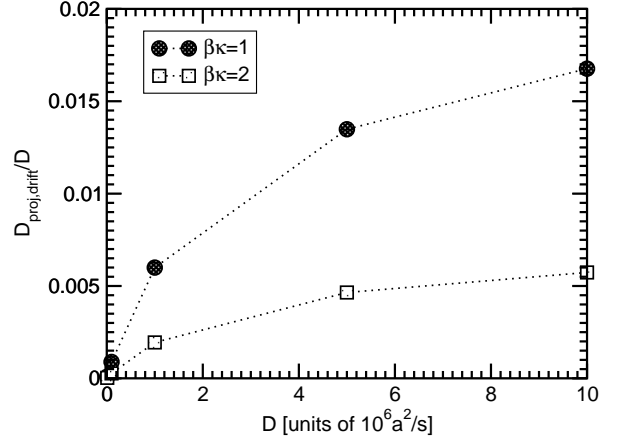


FIG. 9: Additional contribution $D_{\text{proj,drift}}/D$ following from linear fits to $\langle \Delta \mathbf{R}_{\text{drift}}^2(t) \rangle$, see fig. 8, as a function of D for $\beta\kappa = 1, 2$.

can be seen in fig. 5. While our simulation scheme is able to achieve an accuracy of a few percent within reasonable computing time, the corrections caused by the drift term cannot be identified directly via the mean square displacement of the particles. Nevertheless, the explicit evolution of the membrane shape and particle position make it possible to estimate this correction via the evaluation of correlation functions.

VII. CONCLUSIONS

In this paper we introduce a novel scheme that allows for the simultaneous simulation of membrane fluctuations and intramembrane diffusion. The dynamics of the system is expressed via the equation of motion for a membrane described in the Monge gauge and the Langevin equation for a particle diffusing along a surface whose form is given in the Monge gauge. The simulation algorithm consists of the numerical integration of these two coupled differential equations. To validate the membrane fluctuations we compare the height-height correlation function determined from the simulations with known analytical results. After ensuring that membrane fluctuations are reproduced correctly we study free membrane bound diffusion along the membrane. Since diffusion coefficients are experimentally often determined from the projected path a particle covers, we regard the ratio of the measured, projected diffusion coefficient and the intramembrane diffusion coefficient that is a parameter of the simulations and calculations. Both the simulations and the previous calculations that apply a preaveraging approximation, show that the difference between the measured and the true intramembrane diffusion coefficient is largest for small bending rigidities κ and small effective surface tensions σ . This can be understood because small κ and σ lead to stronger membrane fluctuations. Thus the actual path and the projected path differ most. Our calculations reveal a maximum reduction of the projected diffusion coefficient by approximately 20 percent. We are aware that the experimental corroboration of our findings is currently

challenging, but with the constantly increasing accuracy of methods to determine lateral diffusion it should become feasible in the near future. Such experiments will be important in showing that lateral diffusion is not only a function of the direct interaction of lipids and proteins but also depends on material properties of the membrane.

We also consider simulation runs with different intramembrane diffusion coefficients D . The subsequent analysis reveals a surprising observation: the resulting ratios D_{proj}/D all coincide independently of D . Furthermore, the simulation results agree well with the analytical preaveraging calculations. Only simulation runs with the smallest regarded diffusion coefficients D are expected to be well described by the analytical results. For the largest used D , however, when diffusive and membrane time scales become comparable, one would a priori assume that the ratio D_{proj}/D from the explicit simulations would differ from the calculations.

An analysis of the Langevin equation that determines the movement of the particle, demonstrates that correlations of the drift term caused by the metric of the membrane are responsible for a possible increase in the measured diffusion coefficient. In order to understand the applicability of the preaveraging approximation we study these correlation functions using our simulation scheme. The relevant correlations decrease in time not only due to membrane fluctuations but also due to the movement of the particle. Our simulations reveal that the influence of the drift term on the projected diffusion coefficient increases with increasing D . But surprisingly for all, even infinite, intramembrane diffusion coefficients it is very weak in experimentally accessible membranes. In fact the influence is so small – in our simulations below two percent –, that it cannot be directly identified from studying the mean square displacement of the particles within our scheme. Only the study of the correlation functions of the drift term using our simulations gives insight into the additional contributions to the projected diffusion coefficient. For future studies one

may now argue that preaveraging suffices and the simulation scheme becomes unnecessary. Note that this reasoning only makes sense as long as the particle diffuses freely. If an additional interaction between membrane and protein is included the analytical calculation of both the altered diffusion coefficient and membrane spectrum relies on approximations which the simulations are capable of overcoming.

The experimental study of lateral diffusion in membranes has become a very important and much noticed field that has revealed many different diffusion phenomena. But so far only little complementing theoretical or simulational work has been performed in order to develop a broader understanding of experimental findings. In previous work [25] we regarded the influence of a simple interaction between a diffusing particle and the membrane curvature and found a strongly altered dependence of the projected diffusion coefficient on bending rigidity and effective tension. It is therefore promising that the measurement of lateral diffusion coefficients as a function of membrane properties might shed light on the interaction between protein and membrane. While our previous calculations employed several approximations the method introduced in this paper overcomes these. Our powerful simulation scheme is, therefore, a good starting point to investigate the influence of various membrane-protein interactions not only on lateral diffusion but also on the spectrum of the membrane. Further effects that are easily incorporated into our scheme are external influences on the membrane, like tethers that resemble the attachment of a membrane to the cytoskeleton. These and other extensions will be part of our future work.

Acknowledgments

The authors thank R. Finken, T. Speck, and O. Farago for helpful discussions.

-
- [1] J. Lippincott-Schwartz, N. Altan-Bonnet, and G. H. Patterson, *Nat. Cell Biol.* **Suppl. 5**, S7 (2003).
- [2] E. A. J. Reits and J. J. Neefjes, *Nat. Cell Biol.* **3**, E145 (2001).
- [3] A. Kusumi, C. Nakada, K. Ritchie, K. Murase, K. Suzuki, H. Murakoshi, R. S. Kasai, J. Kondo, and T. Fujiwara, *Annu. Rev. Biophys. Biomol. Struct.* **34**, 351 (2005).
- [4] T. Kohl and P. Schwill, *Adv. Biochem. Eng. Biot.* **95**, 107 (2005).
- [5] G. Orädd and G. Lindblom, *Spectroscopy* (2005).
- [6] P. H. M. Lommerse, H. P. Spaink, and T. Schmidt, *BBA-Biomembranes* **1664**, 119 (2004).
- [7] B. M. Aizenbud and N. D. Gershon, *Biophys. J.* **38**, 287 (1982).
- [8] R. Hołyst, D. Plewczynski, A. Aksimentiev, and K. Burdzy, *Phys. Rev. E* **60**, 302 (1999).
- [9] D. Plewczynski and R. Hołyst, *J. Chem. Phys.* **113**, 9920 (2000).
- [10] J. Balakrishnan, *Phys. Rev. E* **61**, 4648 (2000).
- [11] J. Farauto, *J. Chem. Phys.* **116**, 5831 (2002).
- [12] M. Christensen, *J. Comp. Phys.* **201**, 421 (2004).
- [13] P. Schwartz, D. Adalsteinsson, P. Colella, A. P. Arkin, and M. Onsum, *Natl. Acad. Sci. USA* **102**, 11151 (2006).
- [14] I. F. Sbalzarini, A. Hayer, A. Helenius, and P. Koumoutsakos, *Biophys. J.* **90**, 878 (2006).
- [15] F. Brochard and J. F. Lennon, *J. Phys. (Paris)* **11**, 1035 (1975).
- [16] U. Seifert, *Adv. Phys.* **46**, 13 (1997).
- [17] L. C.-L. Lin and F. L. H. Brown, *Phys. Rev. Lett.* **93**, 256001 (2004).
- [18] L. C.-L. Lin and F. L. H. Brown, *Biophys. J.* **86**, 764 (2004).
- [19] R.-J. Merath and U. Seifert, *Phys. Rev. E* **73**, 010401(R) (2006).
- [20] N. Gov, A. G. Zilman, and S. Safran, *Phys. Rev. Lett.* **90**, 228101 (2003).
- [21] L. C.-L. Lin, N. Gov, and F. L. H. Brown, *J. Chem. Phys.* **124**, 074903 (2006).
- [22] L. C.-L. Lin and F. L. H. Brown, *Phys. Rev. E* **72**, 011910 (2005).
- [23] B. Halle and S. Gustafsson, *Phys. Rev. E* **55**, 680 (1997).
- [24] S. Gustafsson and B. Halle, *J. Chem. Phys.* **106**, 1880 (1997).
- [25] E. Reister and U. Seifert, *Europhys. Lett.* **71**, 859 (2005).
- [26] N. S. Gov, *Phys. Rev. E* **73**, 041918 (2006).
- [27] P. B. Canham, *J. theoret. Biol.* **26**, 61 (1970).

- [28] W. Helfrich, *Z. Naturforsch. C* **28**, 693 (1973).
- [29] S. A. Safran, *Statistical Thermodynamics of Surfaces, Interfaces, and Membranes* (Perseus Books, 2003).
- [30] M. Doi and S. F. Edwards, *The Theory of Polymer Dynamics* (Oxford University Press, 1986).
- [31] M. Raible and A. Engel, *Appl. Organometal. Chem.* **18**, 536 (2004).
- [32] H. Risken, *The Fokker-Planck Equation* (Springer-Verlag Berlin Heidelberg, 1996), 2nd ed.
- [33] M. Frigo and S. G. Johnson, *Proceedings of the IEEE* **93**, 216 (2005).